Crystal Structure of the [(C₅H₄BMe₂)₂Fe]-4,4′-bipyridine Polymer from High Resolution X-Ray Powder Diffraction

$$\text{Crystal Structure of the } [(C_5H_4BMe_2)_2Fe]\text{-4,4′-bipyridine Polymer}$$
$$\text{from High Resolution X-Ray Powder Diffraction}$$

Robert E. Dinnebier[a]*, **Matthias Wagner[b], Frank Peters[c], Kenneth Shankland, and William I. F. David[d]**

[a] Bayreuth, Laboratory of Crystallography, University of Bayreuth

[b] Frankfurt(Main), Department of Inorganic Chemistry, J. W. Goethe University

[c] Leverkusen, Bayer AG

[d] Chilton, Didcot, Oxon/UK, ISIS Facility, Rutherford Appleton Laboratory

Abstract. The crystal structure of $[(C_5H_4BMe_2)_2Fe]$-4,4′-bipyridine $[\mathbf{2} \cdot \text{bipy}]_n$ has been determined by the method of simulated annealing from high resolution X-ray powder diffraction at room temperature. The compound is of interest, because it proves that highly ordered organometallic macromolecules can be formed in the solid state via the self-assembly of N–B-donor-acceptor bonds. $[\mathbf{2} \cdot \text{bipy}]_n$ crystallizes in the triclinic space group, $P\bar{1}$, $Z = 2$, with unit cell parameters of $a = 8.3366(2)$ Å, $b = 11.4378(3)$ Å, $c = 12.6740(5)$ Å, $\alpha = 112.065(2)°$, $\beta = 108.979(1)°$, $\gamma = 90.551(2)°$, and $V = 1047.06(6)$ Å³. For the structure solution of $[\mathbf{2} \cdot \text{bipy}]_n$ 11 degrees of freedom (3 translational, 3 orientational, 5 torsion angles) were determined within several hours, demonstrating that the crystal packing and the molecular conformation of medium sized (< 50 non-hydrogen atoms) coordination compounds can nowadays be solved routinely from high resolution powder diffraction data.

Keywords: Powder Diffraction; Simulated annealing; N–B-donor-acceptor bonds; Organometallic polymer

Die Kristallstruktur des Polymers [(C₅H₄BMe₂)₂Fe]-4,4′-Bipyridin mittels hochaufgelöster Röntgenpulverbeugung

Inhaltsübersicht. Die Kristallstruktur von $[(C_5H_4BMe_2)_2Fe]$-4,4′-bipyridine $[\mathbf{2} \cdot \text{bipy}]_n$ wurde mittels der Methode des Simulated Annealing aus hochauflösenden Röntgenbeugungsaufnahmen an Pulvern bei Raumtemperatur gelöst. Die Verbindung ist von Interesse, da sie beweist, daß sich hoch geordnete metallorganische Makromoleküle über N–B-Donor-Akzeptor Bindungen im Festkörper bilden können. $[\mathbf{2} \cdot \text{bipy}]_n$ kristallisiert in der triklinen Raumgruppe $P\bar{1}$ $(Z = 2)$ mit Gitterparametern von $a = 8.3366(2)$ Å, $b = 11.4378(3)$ Å, $c = 12.6740(5)$ Å, $\alpha = 112.065(2)°$, $\beta = 108.979(1)°$, $\gamma = 90.551(2)°$ und $V = 1047.06(6)$ Å³. Bei der Kristallstrukturbestimmung von $[\mathbf{2} \cdot \text{bipy}]_n$ wurden 11 Freiheitsgrade (3 der Translation, 3 der Rotation und 5 Torsionswinkel) innerhalb einiger Stunden bestimmt, womit gezeigt werden kann, daß Kristallpackung und Molekülkonformation mittelgroßer Koordinationsverbindungen (< 50 Nicht-Wasserstoff Atome) heutzutage routinemäßig aus hochauflösenden Pulverbeugungsdaten gelöst werden können.

Introduction

The electronic and magnetic interactions between transition metal atoms in solid organometallic materials depend on the distance and relative orientation of these metals in the crystal lattice, as well as on the chemical nature of the bridging ligands. Therefore, current vivid research focuses on the development of concepts for the design of metal-containing macromolecular chains, networks and even three-dimensional assemblies. One obvious strategy is to start from mononuclear transition metal complexes as elementary units, which are then connected to form the desired multinuclear arrays. If the individual building blocks possess a well-known and rigid structure, this approach even provides a chance to predict to some degree the crystal lattice of the resulting material. In this context, the availability of a highly efficient linking mechanism with a low activation energy barrier is of prime importance to avoid lattice defects. Some well-established procedures rely on the interaction of coordinatively unsaturated transition metal complexes with (at least) bifunctional Lewis-bases. In other cases, hydrogen-bridge donors and -acceptors are fixed at the periphery of metal complexes, so that macromolecular entities can be established by the cooperative action of the resulting weak hydrogen bonds.

It has been suggested recently [1, 2] that organometallic compounds bearing Lewis-acidic boron substituents may also serve as promising building blocks for the formation of supramolecular aggregates, since they can easily be linked by amines or phosphines via B–N(P) adduct bonds. Following this approach, the di-

* Dr. Robert E. Dinnebier
Laboratory of Crystallography
University of Bayreuth
D-95440 Bayreuth
Germany
E-mail: robert.dinnebier@uni-bayreuth.de

nuclear adduct **1** · bipy · **1** and the polymeric compound [**2** · bipy]$_n$ (Scheme 1) have been obtained from borylated ferrocenes and the bifunctional amine 4,4′-bipyridine (bipy).

1 · bipy · 1
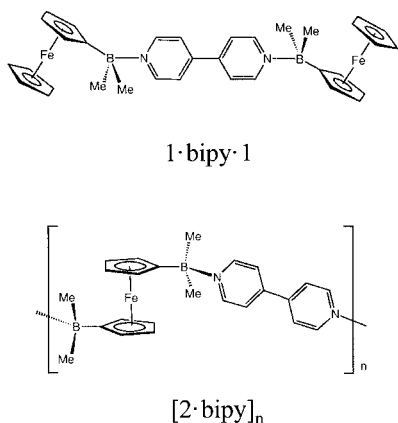
[2 · bipy]$_n$

Scheme 1

Solid [**2** · bipy]$_n$ showed a surprisingly high thermal stability and was reasonably inert toward air and moisture. Moreover, the compound possesses an unusual dark purple color, which indicates charge-transfer interactions to occur along the polymer backbone [1, 2]. Unfortunately, the main proof for the macromolecular nature of [**2** · bipy]$_n$ had to rest on a qualitative end-group determination by infrared spectroscopy. Due to the poor solubility of [**2** · bipy]$_n$ most of the established tools for polymer analysis were not applicable and all attempts to synthesize single crystals of [**2** · bipy]$_n$ suitable for single crystal diffraction failed. Therefore, the crystal structure of [**2** · bipy]$_n$ was solved *ab initio* from high resolution powder pattern using the method of simulated annealing [e. g. 3].

The complexity and accuracy of crystal structure refinements from powder data has been growing steadily since the pioneering work of *Hugo Rietveld* about 30 years ago [4]. Nowadays, even the crystal structures of small proteins can be refined from high resolution powder data [5]. On the other hand, it took another 20 years before a considerable number of structure determinations from powder diffraction data appeared in the literature [6]. Most of these early "powder structures" were solved by applying traditional structure solving methods known from single crystal analysis to powder data of inorganic solids. With the occurrence of real space methods about 10 years ago it became possible to determine the crystal structure of molecular compounds [6]. As a prerequisite for the successful application of real space methods, the connectivity within a group of atoms must be known prior to structure determination, which is usually the case for molecules.

Among the first direct space algorithms were more or less sophisticated grid searches. Random (i. e. Monte Carlo) techniques significantly outperform such grid searches and have allowed structures with around 7 degrees of freedom to be determined [e. g. 7–10]. Hence they were used mainly for rigid molecules with few internal degrees of freedom. Simulated annealing was a logical extension of these simple MC approaches [11–18] allowing the crystal structure determination of fairly complex molecular compounds with several internal degrees of freedom (torsion angles) and several molecules in the asymmetric unit. Recent advances in this field lie in the treatment of overlapping reflections, the development of faster algorithms and better annealing schedules [13]. Among the various alternative approaches is the minimization of the lattice energy [19]. This method depends strongly on the quality of the potential parameters and the available computing power.

The main focus of this study will be on the structure elucidation by the simulated annealing technique and the consecutive Rietveld analysis from synchrotron X-ray powder data. This is one of the first examples where the previously unknown crystal structures of such a complex compound as [**2** · bipy]$_n$ could be solved from X-ray powder data applying a routine procedure.

Experimental Section

Synthesis, spectroscopical investigations and thermal analysis of [**2** · bipy]$_n$ have been published elsewhere [1].

For the high resolution X-ray powder diffraction experiments, the sample was sealed in a glass capillary of 0.7 mm diameter (Hilgenberg glass No. 50). Powder diffraction data were collected at room temperature at beamline X3B1 at the National Synchrotron Light Source, Brookhaven National Laboratory (Tab. 1). X-ray wavelengths were selected by a double Si(111) monochromator and they were calibrated with the NBS1976 alumina standard. The diffracted beam was analyzed with a Ge(111) crystal and detected with a Na(Tl)I scintillation counter with a pulse-height discriminator in the counting chain. The intensity of the primary beam was monitored by an ion chamber. In this parallel beam geometry, the resolution is determined by the analyzer crystal instead of by slits [20].

X-ray scattering intensities were recorded at wavelength 0.82488(2) Å) for 5.1 seconds at each 2θ in steps of 0.004° from 3.0° to 34.448° (Fig. 1). The sample was spun around θ during measurement to reduce crystallite-size effects. Lowest angle diffraction peaks had a full width at half maximum (FWHM) of 0.011°2θ, close to the resolution of the diffractometer. Data reduction was performed using the program GUFI 5.0 [21]. Indexing of the powder pattern of [**2** · bipy]$_n$ using the program ITO [22] led to a primitive triclinic unit cell with lattice parameters given in Tab. 1. The lattice can also be regarded as pseudo-monoclinic with a deviation of approx. 0.5° from 90° angle. The number of formula units per unit cell could be determined to Z = 2 from packing considerations, indicating $P\bar{1}$ as the most probable space group, which could later be confirmed by Rietveld refinement.

The peak profiles and precise lattice parameters were determined by LeBail-type fits using the program Fullprof

Z. Anorg. Allg. Chem. **2000**, *626*, 1400–1405

1401

Table 1 Crystallographic data for [**2** · bipy]$_n$

formula	$FeB_2N_2C_{24}H_{29}$
temperature/K	295
formula weight/gmol^{-1}	422.98
space group	$P\bar{1}$
a/Å	8.3366(2)
b/Å	11.4378(3)
c/Å	12.6740(5)
α/°	112.065(2)
β/°	108.979(1)
γ/°	90.551(2)
V/Å^3	1047.06(6)
Z	2
calc. Density/g cm^{-3}	1.34
μ/cm^{-1}	26.65
2θ range/°	2.0–34.448
step size/°	0.004
counting time per step/s	5.1
Wavelength/Å	0.82488(2)

Table 2 Positional parameters of [**2** · bipy]$_n$ in $P\bar{1}$ symmetry at 295 K. All temperature factors are constrained to be equal within the molecule (4.61(8) Å^2)

atom	x/a	y/b	z/c
B(1)	.6057(26)	.2748(18)	.2492(19)
C(2)	.3956(26)	.2463(18)	.1773(21)
C(1)	.6602(35)	.2050(20)	.3452(20)
C(11)	.7457(19)	.2459(20)	.1770(12)
N(1)	.6896(14)	.4392(13)	.3400(19)
C(31)	.7345(14)	.4893(24)	.4652(20)
C(32)	.7733(15)	.6223(27)	.5347(12)
C(33)	.7702(15)	.7090(14)	.4810(21)
C(34)	.7237(15)	.6610(24)	.3532(21)
C(35)	.6893(14)	.5271(25)	.2872(11)
C(43)	.8030(18)	.8493(13)	.5536(24)
C(42)	.7250(15)	.9280(24)	.4965(13)
C(41)	.7531(15)	.0669(23)	.5644(20)
N(2)	.8498(17)	.1310(12)	.6931(12)
C(45)	.9216(14)	.0528(12)	.7478(12)
C(44)	.9039(16)	.9115(24)	.6817(23)
C(12)	.7080(21)	.1180(18)	.0929(12)
C(13)	.8337(28)	.0960(15)	.0374(12)
C(14)	.9446(13)	.2123(24)	.0834(13)
C(15)	.8908(29)	.3044(12)	.1695(11)
FE(1)	.7015(7)	.2277(5)	–.0075(6)
C(24)	.6972(15)	.2614(23)	–.1544(12)
C(23)	.5809(31)	.1494(12)	–.1900(11)
C(22)	.4542(20)	.1861(23)	–.1365(12)
C(21)	.4932(22)	.3175(22)	–.0671(12)
C(25)	.6492(32)	.3635(11)	–.0731(11)
B(2)	.8827(34)	.2939(18)	.7829(22)
C(4)	.0626(26)	.3321(19)	.8870(22)
C(3)	.7778(28)	.3589(21)	.6959(20)

[23]. The background was modeled manually using GUFI. The peak-profile was described by a pseudo-Voigt in combination with a special function that accounts for the asymmetry due to axial divergence [24].

Structure solution of [**2** · bipy]$_n$ was tried by direct methods using the program SIRPOW [25]. All attempts failed, using different sets of starting parameters. This can be understood in view of massive accidental overlap of peaks, typical for a unit cell of that size with low space group symmetry.

Since the connectivity of the atoms was known from a single crystal study of a similar compound [2], structure determination for [**2** · bipy]$_n$ was carried out by means of the simulated annealing technique. For the simulated annealing runs, the program DASH [26] was used. Three input files were needed: a description of the connectivity of the molecules including possible torsion angles, a list of diffraction peak intensities, and a list of parameters to be varied and their ranges for the simulated annealing runs.

For the definition of the connectivity between the atoms within the molecule, we used the Z-matrix notation [e. g. 27], which allows for the description of the entire molecule and its intramolecular degrees of freedom by using interatomic distances, angles and dihedral angles. A flag after each parameter determined whether this parameter was included in the simulated annealing process or not. All intramolecular angles and distances were kept fixed at standard values, allowing only the 5 torsion angles to vary (Fig. 2).

The diffraction intensities were extracted from a Pawley type refinement, using the program DASH [28, 26]. The peak profile was modeled by the Voigt-function to which a correction for the asymmetry due to axial divergence was applied. The background was included in the refinement process using high order Chebyshev polynoms. The covariance matrix of the Pawley fit which describes the degree of correlation between the individual intensities of neighboring reflections was actively used in the calculation of the level of agreement between the measured intensities and those of the trial structures after each simulated annealing. It was therefore not necessary to include the entire powder pattern in the simulated annealing procedure which considerably decreased the computing time needed for each cycle. The Pawley fit converged to a χ^2 value of 10.46 for 5501 observations, indicating a reasonable fit to the measured data.

A total of 12 parameters was varied during the simulated annealing runs (5 torsion angles, 3 fractional parameters for the position of the molecule and 4 quaternians [27] describing the orientation of the molecule within the unit cell). The trial structures were generated using a set of numbers chosen randomly in a Monte Carlo fashion within the given range for the 12 parameters [29]. The starting temperature[1]) for the simulated annealing run was set to 100 K, and decreased slowly (Fig. 3), allowing 7200 moves per temperature. Figure 3 shows that the integrated intensities χ^2 value falls dramatically in the first few thousand moves, indicating that the scattering is dominated by the positioning of the Fe atom. By the time the temperature had fallen to 7.34 K, the χ^2 for the integrated intensities had fallen to only 47.7. Several million trial structures were generated before this minimum was reached, the process taking a few hours to run on a Digital Personal Workstation 433 au. A simplex search at the end of the simulated annealing run confirmed that a deep minimum, corresponding to an approximately correct crystal structure, had been obtained. Note that no special algorithms were employed to prevent close contact of molecules during the global optimization procedure. In general, these have not been found to be necessary as the fit to the structure factors alone quickly moves the molecules to regions of the unit cell where they do not grossly overlap with neighbouring molecules.

---

[1]) Temperature is not a temperature in thermodynamical sense but refers to the term T in the expression $\exp\left(\dfrac{E}{KT}\right)$ which is generally known as the Boltzmann factor with the Boltzmann constant K and the state of energy E. The analogous expression with $E = \chi^2_{new} - \chi^2_{old}$ (difference in χ^2 of consecutive cycles) is used as an acceptance criterion in the simulated annealing process.
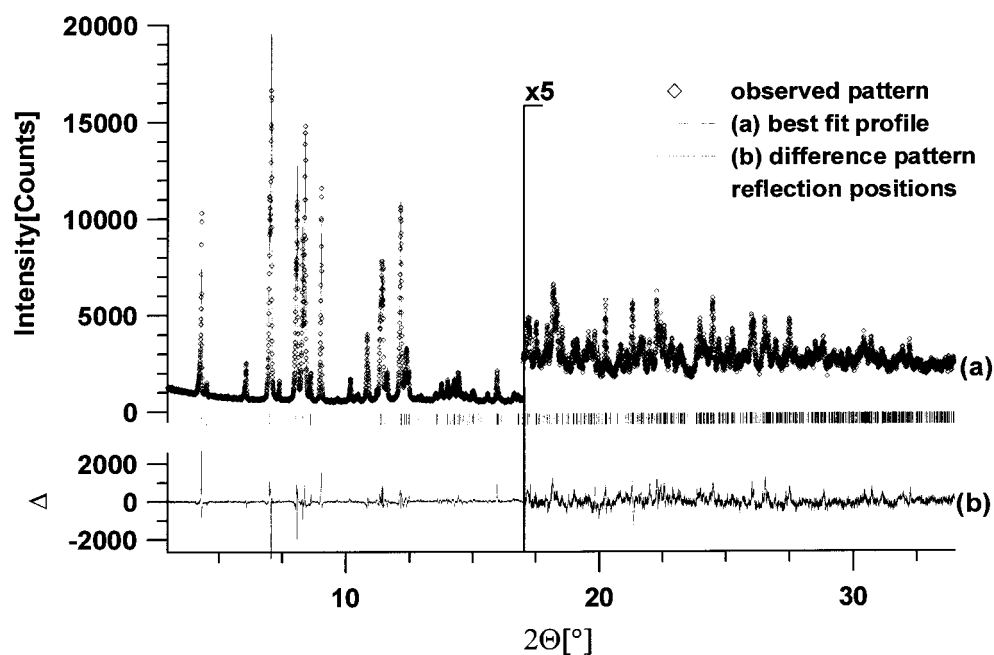
Fig. 1 Scattered X-ray intensity for $[(C_5H_4BMe_2)_2Fe]$-4,4′-bipyridine at ambient conditions as a function of diffraction angle 2θ. Shown are the observed pattern (diamonds), the best Rietveld fit profile (line), the reflection positions and the difference curve between observed and calculated profiles as the trace at the bottom. The high angle part is enlarged by a factor of 5 starting at 17° 2θ. The wavelength was $\lambda = 0.82488(2)$ Å. The R-values are R-p = 6.3%, R-wp = 8.4%, R-F = 8.9%, R-F² = 12.9%. R-p, R-wp, R-F and R-F² refer to the Rietveld criteria of fit for profile, weighted profile, and structure factor, respectively, defined in [32].
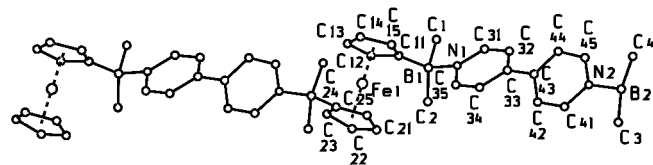
Fig. 2 Molecular structure of two connected $[(C_5H_4BMe_2)_2Fe]$-4,4′-bipyridine units, showing the polymerization.

Preliminary Rietveld refinements were carried out, in which only the scale and overall temperature factors were refined. The unsatisfactory agreement between the measured and the calculated profile indicated that further refinement of bond lengths and bond angles was necessary. Therefore, the coordinates obtained by the simulated annealing techniques were used as starting parameters for Rietveld refinements using the GSAS program system [30]. Since unconstrained refinement resulted in severe distortions from the ideal molecular symmetry, 62 soft constraints were introduced, 36 restraints on bond lengths (weight factor of 30), 4 restraints on the planarity (weight factor of 100) and 22 constraints on bond angles (weight factor of 40) for two pyridine and the two cyclopentadienyl rings. The Rietveld refinement converged quickly to the R-values given in the caption of Fig. 1.

Hydrogen atoms were not included in the refinement process. The positional parameters of the final Rietveld refinement and the overall temperature factor are presented (Tab. 2). It should be noted that the powder pattern of $[2 \cdot bipy]_n$ exhibits some anisotropic peak broadening caused
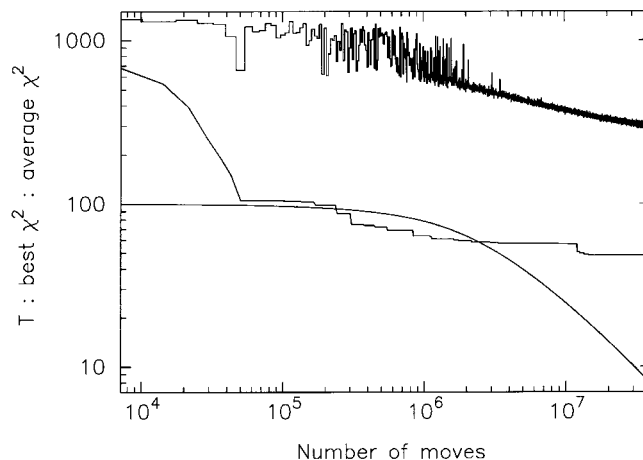

Fig. 3 Progress of the simulated annealing run of $[(C_5H_4BMe_2)_2Fe]$-4,4′-bipyridine, showing the average χ^2 (upper curve), the best χ^2 (middle curve), and the temperature (lower curve) in dependence of the number of moves.

by lattice strain with the sharpest peaks along [010] direction which could be satisfactory modeled by the uniaxial strain model in GSAS.

Results and Discussion

The X-ray powder diffraction data provide conclusive evidence for the polymeric nature of $[2 \cdot bipy]_n$ in the solid state. *Catena*-$[2 \cdot bipy]_n$ consists of long chains,
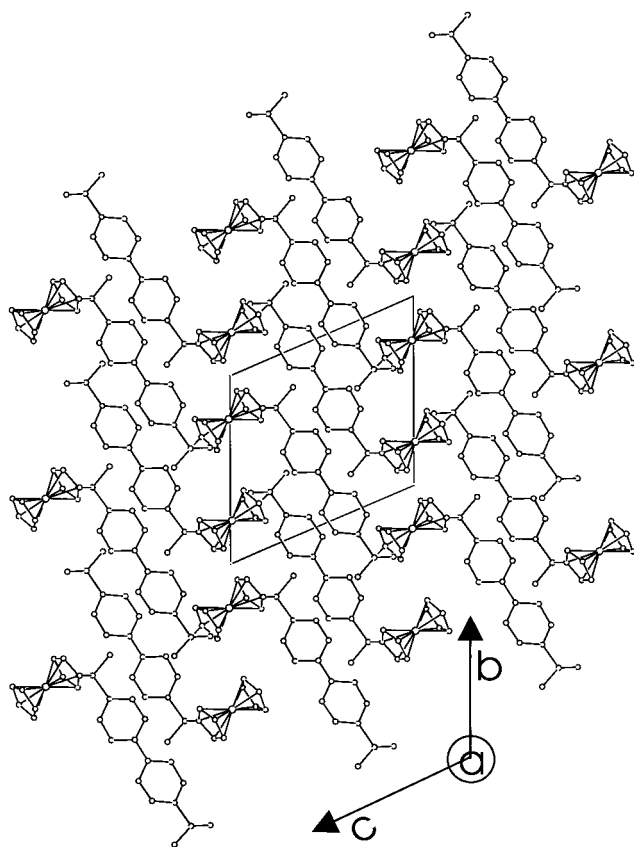
Fig. 4 Crystal structure of [(C$_5$H$_4$BMe$_2$)$_2$Fe]-4,4′-bipyridine. Representation of the packing of the molecules in a projection along *a*-axis.

Table 3 Selected bond lengths/Å, angles/°, and torsion angles/° of [2 · bipy]$_n$ Realistic standard deviations according to ref. 32 are on the order of 1° for the angles and 0.1 Å for the bond lengths

π(Py)–C(33)–C43)-π(Py)	25.7
B–Cp(centroid)-Cp*(centroid)-B*	155.4
C(11)–B(2)–N(2)	96.1
C(24)–B(2)–N(2)	88.7
C(12)–C(11)–B(1)–N(1)	1.3
C(25)–C(24)–B(2)–N(2)	2.4
Fe–Fe intramolecular	13.5
Fe–Fe intermolecular	7.8
B-π(Cp)–Fe	95.4, 94.1
C(11)–B(1)–B(2)–C(3)	45.0
C(1)–B(1)–B(2)–C(4)	44.6

held together by B–N-adduct bonds (Figs. 1, 4). Cyclic structures *cyclo*-[2 · bipy]$_n$, that previously have also been taken into consideration [1] can now safely be ruled out.

The 4,4′-bipyridine bridges in [2 · bipy]$_n$ are twisted by 25.7° about the C(33)–C(43) axis (Fig. 2) while the dinuclear reference system 1 · bipy · 1 was shown to possess a perfectly planar 4,4′-bipyridine unit [1]. As has been stated above, [2 · bipy]$_n$ shows very deep purple color in the solid state, what is highly unusual for ferrocene derivatives and can most likely be attributed to charge transfer interactions between the electron-rich ferrocene donors and the electron-poor 4,4′-bipyridine adduct bridges [1]. This interpretation is in accordance with the observed conformation of the 4,4′-bipyridine linker, which is still sufficiently close to planarity to maintain a high degree of electron delocalization, thereby supplying a LUMO of low energy. On the other hand, the HOMO of the ferrocene donor has been shown to rise in energy as a result of B–N adduct formation [1].

All ferrocene moieties of [2 · bipy]$_n$ adopt an eclipsed conformation with torsion angles B–Cp(centroid)-Cp*(centroid)-B* of 155.4°. The B–N bonds of

[2 · bipy]$_n$ are all located in the plane of their adjacent C$_5$H$_4$ rings (torsion angle C(12)–C(11)–B(1)–N(1) = 1.3°).

In contrast, the analogous torsion angle in 1 · bipy · 1 was found to posses values of 90.5(4)° and 88.6(3)° (two crystallographically independent molecules in the asymmetric unit) [1]. Thus as indicated in Scheme 1, 1 · bipy · 1 and [2 · bipy]$_n$ exhibit significantly different conformations of their N–B–Cp fragments.

In the crystal lattice, the individual polymer chains are piled up in such a way, that discrete stacks of ferrocene- and 4,4′-bipyridine fragments are formed (Fig. 4). The shortest intermolecular Fe–Fe distance was determined to be 7.8 Å, while the shortest intramolecular Fe–Fe distance amounts to 13.5 Å.

It has been shown that a moderately complex crystal structure of a coordination compound can nowadays be routinely solved from high resolution powder diffraction data. The time for structure solution is typically on the order of several hours. Despite these great advances, one has to be aware of the limitations of the powder method, due to systematic and accidental peak overlap in the powder pattern. The latter is severe in the present case. It is indisputably possible to determine the molecular conformations with fairly high precision, but it is usually not possible to determine individual bond lengths and angles within the molecules. This can be seen when comparing bond lengths and angles of [2 · bipy]$_n$ to the corresponding values of 1 · bipy · 1 and similar crystal structures as obtained from single crystal analysis. Maximum deviations of up to 0.1 Å are common, prohibiting chemical interpretation of individual bond length. The deviations result from meaningless shifts of positional parameters caused by the lack of precision of the individual structure factors in the case of powder data. For this reason, only bond lengths, bond angles and torsion angles which define the molecular conformation and the packing of the molecules are presented (Tab. 3). All other bond lengths and angles have been deposited as supplementary data and will not be discussed in this paper.

References

[1] M. Fontani, F. Peters, W. Scherer, W. Wachter, M. Wagner, P. Zanello, *Eur. J. Inorg. Chem.* **1998**, 1453; M. Fontani, F. Peters, W. Scherer, W. Wachter, M. Wagner, P. Zanello, *ibid.* 2087.

[2] M. Grosche, E. Herdtweck, F. Peters, M. Wagner, *Organometallics* **1999**, *18*, 4669.

[3] P. J. M. van Laarhoven, E. H. L. Aarts, *Simulated Annealing: Theory and Applications*, D. Reidel Publishing Company, Dordrecht 1987.

[4] H. M. Rietveld, *J. Appl. Crystallogr.* **1969**, *2, 65.*

[5] R. B. Von Dreele, *J. Appl. Crystallogr.* **1999**, *32*, 1084.

[6] A. LeBail, *Structure Determination from Powder Diffraction – Database.* http://fluo.univ-lemans.fr:8001/iniref.html 1999, website.

[7] V. V. Chernyshev, H. Schenk, *Z. Kristallogr.* **1998**, *213*, 1.

[8] N. Masciocchi, M. Moret, P. Cairati, F. Ragaini, A. Sironi, *J. Chem. Soc., Dalton Trans.* **1993**, 473.

[9] G. M. Bendele, P. Stephens, K. Prassides, K. Vavekis, K. Kordatos, K. Tanigaki, *Phys. Rev. Letters* **1998**, *80(4)*, 736.

[10] R. E. Dinnebier, P. W. Stephens, J. K. Carter, A. N. Lommen, P. A. Heiney, A. R. McGhie, L. Brard, A. B. Smith, III, *J. Appl. Cryst.* **1995**, *28*, 327.

[11] J. M. Newsam, M. W. Deem, C. M. Freeman, *Accuracy in Powder Diffraction II, NIST Spec. Publ. No. 846* **1992**, 80.

[12] Y. G. Andreev, G. S. MacGlashan, P. G. Bruce, *Phys. Rev. B* **1997**, *55(18)*, 12011.

[13] W. I. F. David, K. Shankland, N. Shankland, *Chem. Commun.* **1998**, 931.

[14] M. Tremayne, B. M. Kariuki, K. D. M. Harris, *J. Appl. Crystallogr.* **1996 a**, *29*, 211.

[15] M. Tremayne, B. M. Kariuki, K. D. M. Harris, *J. Mater. Chem.* **1996 b**, *6(9)*, 1601.

[16] M. Tremayne, B. M. Kariuki, K. D. M. Harris, *Angew. Chemie* **1997**, *109*, 788; *Angew. Chem. Int. Ed.* **1997**, *36*, 770.

[17] Y. G. Andreev, P. G. Bruce, *J. Chem. Soc., Dalton Trans.* **1998**, 4071.

[18] G. S. MacGlashan, Y. G. Andreev, P. G. Bruce, *Nature* **1999**, *398*, 792.

[19] M. U. Schmidt, R. E. Dinnebier, *J. Appl. Crystallogr.* **1999**, *32*, 178.

[20] D. E. Cox, Handbook on Synchrotron Radiation, Vol. 3, chapter 5 Powder Diffraction, eds G. Brown & De. E. Moncton, Elsevier Science Publishers B.V. 1991.

[21] R. E. Dinnebier, L. W. Finger, *Z. Kristallogr. Suppl.* **1998**, *15*, 148.

[22] J. W. Visser, *J. Appl. Crystallogr.* **1969**, *2*, 89.

[23] J. Rodriguez-Carvajal, *Abstracts of the Satellite Meeting on Powder Diffraction of the XV Congress of the IUCr, Toulouse, France* **1990**, 127.

[24] L. W. Finger, D. E. Cox, A. P. Jephcoat, *J. Appl. Crystallogr.* **1994**, *27*, 892.

[25] G. Cascarano, L. Favia, C. Giacovazzo, *J. Appl. Crystallogr.* **1992**, *25*, 310.

[26] W. I. F. David, Simulated annealing program DASH **1999**, personal communication.

[27] A. R. Leach, *Molecular Modelling Principles and Applications*, Addison Wesley Longman Limited 1996, p. 2.

[28] G. S. Pawley, *J. Appl. Crystallogr.* **1981**, *14*, 357.

[29] W. H. Press, S. A. Teukolsky, W. T. Vetterling, B. P. Flannery, *Numerical Recipes in Fortran 77*, 2nd ed., Cambridge University Press 1992.

[31] A. C. Larson, R. B. Von Dreele, *„GSAS – General Structure Analysis System"*, Los Alamos National Laboratory Report LAUR 86-748 **1994**, available by anonymous FTP from ftp://ftp.lanl.gov./public/gsas.

[32] I. Langford, D. Louër, *Rep. Prog. Physics.* **1996**, *59*, 131.

Z. Anorg. Allg. Chem. **2000**, *626*, 1400–1405

1405